Synthesis, solid state and solution structures of two isomeric dicopper(II) complexes with functionalized azetidine ligands

Peter Comba · Nina Dovalil · Hyang Hoo Kim ·
Jong Seung Kim · Yang Kim · Young Hoon Lee ·
Pierre Thuéry · Marta Zajaczkowski

Abstract Reported are the crystal and solution structures (determined by X-ray crystallography and EPR spectroscopy/simulation of the EPR spectra, respectively) of two dinuclear Cu^{II} complexes, coordinated to isomeric dinucleating azetidine-based ligands, whose N_3 cavities (pyridine/azetidine/secondary amine) are bridged by para- or meta-substituted phenyl groups. The Cu^{II} sites in the two dinuclear systems are similar to each other and as expected from the known structure of the corresponding mononuclear complex. The significant differences between the crystal structures of the mono- and the two dinuclear complexes and between the crystal and the solution structures are due to the elasticity of the Cu^{II} coordination sphere, the flexibility of the dinucleating ligands and subtle changes related to weak interactions (crystal lattice, solvation, anion coordination/ion pairing).

P. Comba (✉) · N. Dovalil · M. Zajaczkowski
Anorganisch-Chemisches Institut, Universität Heidelberg,
INF 270, 69120 Heidelberg, Germany
e-mail: peter.comba@aci.uni-heidelberg.de

H. H. Kim · Y. Kim (✉)
Department of Chemistry and Advanced Materials,
Kosin University, 149-1, Dongsam-dong, Yeongdo-gu,
Busan 606-701, South Korea
e-mail: ykim@kosin.ac.kr

J. S. Kim · Y. H. Lee
Department of Chemistry, Korea University,
Anam-dong, Seongbuk-Gu, Seoul 136-701, South Korea

P. Thuéry
CEA, IRAMIS, SIS2M, LCCEf (CNRS URA 331),
Bâtiment 125, 91191 Gif-sur-Yvette, France

Introduction

The functionalization of *N*-aminoethyl azetidines has been shown to yield chelate ligands for various transition metal ions with interesting steric and electronic properties [1, 2]. Complexes of *N*-aminoethyl azetidine derivatives have, in comparison with those of primary amines, shorter metal-N (azetidine) bonds than might have been expected [3], that is, azetidine nitrogens are relatively strong σ-donor ligands [4, 5]. In addition they cannot be oxidized to the corresponding imines, and this adds to the redox stability of the corresponding complexes. The tridentate N_3 ligand L^1 was shown to readily coordinate to Cu^{II} with the formation of both mono- and dinuclear complexes [1]. We now report the synthesis and Cu^{II} coordination chemistry of the two related dinucleating bis-tridentate azetidine ligands L^2 and L^3 (see Scheme 1) and analyze their solid state and solution structures in comparison with the mononuclear complex.

Results and discussion

The two dinucleating ligand L^2 and L^3 are obtained in good yield by condensation of the two isomeric phthaladehydes with the tridentate azetidine ligand L^1 and subsequent $NaBH_4$ reduction of the Schiff base ligands.

Reaction of the isophthalaldehyde-bridged ligand L^2 with $CuCl_2 \cdot 2H_2O$ in ethanol yields the blue crystalline complex $[(Cl)_2Cu(L^2)Cu(Cl)(OH)] \cdot H_2O$ (**1**), whose infrared spectra confirm the presence of OH and NH stretching
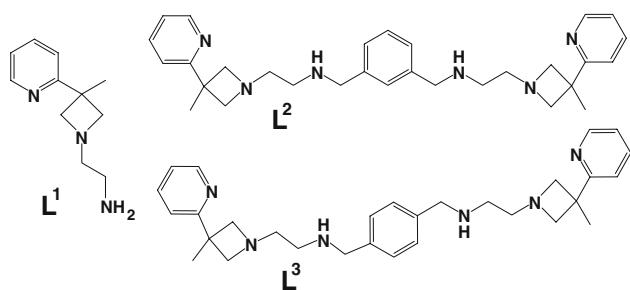
Scheme 1 Ligand structures

bands. The X-ray structure (see Fig. 1; Table 1) shows that **1** is an unsymmetrical dicopper (II) complex. The Cu(1) site exhibits a distorted square pyramidal coordination geometry, with an N_3Cl_2 donor set. The N_3Cl donor set with Cl(1) defines the basal plane with Cl(2) as the axial ligand (Cu(1)–Cl(2) = 2.456 vs. 2.316 Å); the relatively small difference between axial and equatorial Cu–Cl distance is as expected from the considerable distortion towards a trigonal bipyramidal geometry, $\tau = 0.54$; $\tau = 0$ vs. 1 for square planar and trigonal bipyramidal, respectively) [6]. The Cu(2) site also is five-coordinate. There is a rather short bond to an in-plane coordinated chloride *trans* to the azetidine nitrogen (Cu(2)–Cl(3) = 2.297 Å) and an elongated bond to an axial water (Cu(2)–O = 2.478 Å, $\tau = 0.43$). Interestingly, the related mononuclear complex $[(L^1)Cu(Cl)_2]$ [1] also adopts a five-coordinate geometry with an N_3Cl_2 donor set similar to that around Cu(1) but with a coordination geometry closer to trigonal bipyramidal ($\tau = 0.79$, see Table 1).

Reaction of the terephthalaldehyde-bridged ligand L^3 with $CuCl_2 \cdot 2H_2O$ in ethanol and, in contrast to the preparation of the complex with L^2, in presence of an excess of $LiClO_4$, in order to obtain better crystals, yields the blue crystalline complex $[(Cl)(OH_2)Cu_2L^3(OH_2)Cl](CH_3OH)$ $(ClO_4)_2$ (**2**), whose infrared spectrum confirms the presence of OH, NH and ClO_4 stretching bands. The crystal structure (see Fig. 2; Table 1) confirms two symmetry related (identical) Cu^{II} centers, best described as distorted square pyramidal ($\tau = 0.38$). The basal plane is defined by the three nitrogen donors of L^3 and a chloro ligand (Cl(1)),

with a water molecule at the axial position. The varying degrees of trigonal distortion in the two structures of the dinuclear (L^2, L^3) and in the mononuclear complex (L^1) indicate that the coordination geometry is, as expected for Cu^{II}, rather elastic, and the observed energy minimum structures are largely enforced by crystal lattice effects. Obviously, these depend on the molecular structures, and these are related to the two configurations of the dinucleating ligand (L^2 versus L^3).

Weakly dipole–dipole-coupled paramagnetic centers exhibit, due to the coupling of each of the electron spins with both centers relatively complex EPR spectra. Specifically those of dicopper (II) systems with two $S = 1/2$ Cu^{II} ions and $I_{Cu} = 3/2$ have been studied extensively, and the simulation of the spectra has been used to deduce structural information [7]. Therefore, EPR spectroscopy in combination with spectra simulations and, where appropriate, various molecular modeling techniques have been used extensively to determine structures of di- and trinuclear Cu^{II} complexes in solution [8–12]. Since the molecular structures of the complexes **1** and **2** reported here are known in the solid, structure optimization was not thought to be required in the present study, and EPR spectroscopy/spectra simulations have been used to thoroughly analyze the solution structures in comparison with the known crystal structures. Figure 3 shows the experimental and simulated EPR spectra of the mononuclear complex of L^1 [1] and the two dicopper (II) complexes **1** and **2**, based on the isomeric ligands L^2 and L^3; the spin Hamiltonian and structural parameters of the corresponding simulations are given in Table 3. The spectra of the solutions did not change with time, and it therefore appears that the relatively labile monodentate ligands (OH_2, OH^-, Cl^-) are exchanged in solution (aqueous DMF, see Experimental) to yield common coordination spheres (presumably 2 OH_2 donors at each Cu^{II} center in addition to the tridentate chelate provided by the substituted azetidines). It was not expected that the spectra simulations yield various sets of g- and A-tensor parameters (see Table 2), and we interpret this as structural differences enforced by the two isomeric ligands rather than by different co-ligands. That is, in agreement with the observations due to the solid state structures (see above), there is a high elasticity of the Cu^{II}

Fig. 1 ORTEP plot of $[(Cl)_2Cu(L^2)Cu(Cl)(OH)]\cdot H_2O$ (**1**). Displacement ellipsoids are drawn at the 50% probability level. Carbon-bound hydrogen atoms and the solvent molecule are omitted for clarity
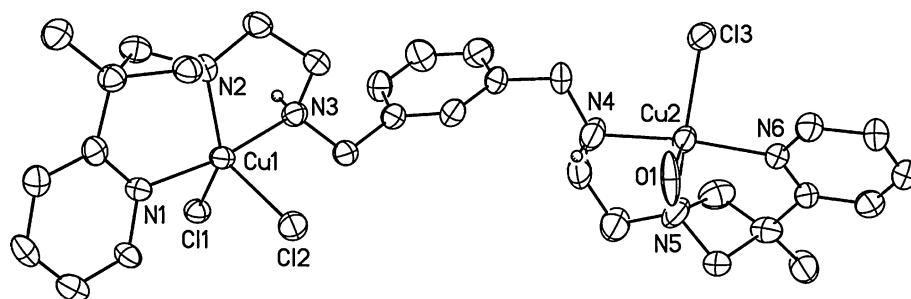
Table 1 Selected structural parameters (distances in Å, angles in °; τ describes the distortion towards a trigonal bipyramid [6])

	$[(L^1)Cu(Cl)_2]$ [1]	$[(L^2)Cu_2(Cl)_3(OH)]$ (**1**)		$[(L^3)Cu_2(Cl)_2(OH_2)_2]^{2+}$ (**2**)	
Cu–Npy	2.05	N(1,6)	2.054(5), 2.043(5)	Cu–N(1,1′)	2.058(4)
Cu–Naz	2.04	N(2,5)	2.043(6), 2.041(7)	Cu–N(2,2′)	2.006(5)
Cu–NH	2.01	N(3,4)	2.019(5), 2.048(6)	Cu–N(3,3′)	2.019(5)
Cu–Cl	2.37, 2.40	Cl(1,3)	2.3161(17), 2.297(2)	Cu–Cl(1,1′)	2.3103(14)
Cu–Cl	–	Cl(2)	2.4557(18)		–
Cu–OH$_{(2)}$	–	O(1)	2.478(5)	Cu–O(1,1′)	2.187(5)
Cu⋯Cu	–		10.07		11.46
Angle (α, β) [°]^a	–		14, 20		0, 0
Npy–Cu–NH	171	N(3-1, 4-6)	172, 170	N(3-1)	170
Npy–Cu–Naz	88	N(2-1, 5-6)	89, 87	N(2-1)	88
NH–Cu–Naz	84	N(3-2, 4-5)	83, 84	N(3-2)	82
Cl–Cu–X	119	Cl$_1$–Cu$_1$–Cl$_2$	110	Cl$_1$–Cu$_1$–O$_1$	94
Cl–Cu–OH$_2$	–	Cl$_3$–Cu$_2$–O$_1$	109	Cl$_1$′–Cu$_1$′–O$_1$′	94
τ	0.79	Cu$_1$, Cu$_2$	0.54, 0.43		0.38

^{a} α is the angle between the *xy* plane of Cu$_1$ and the line connecting Cu$_1$ and Cu$_2$, and β is the angle between the *z* axes of the two local coordinate systems around Cu$_1$ and Cu$_2$
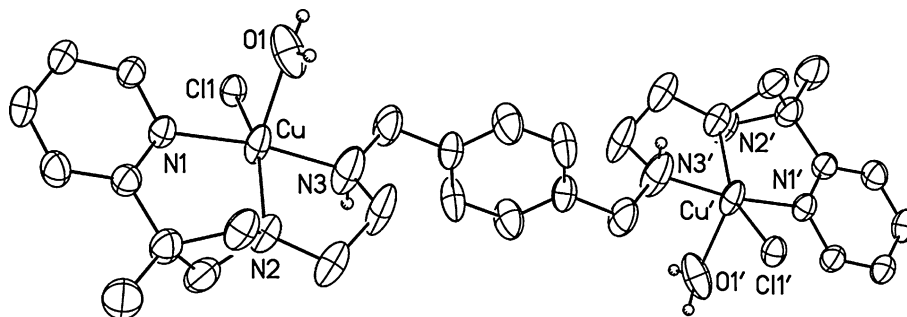

Fig. 2 ORTEP plot of $[(Cl)(OH_2)Cu_2(L^3)(OH_2)(Cl)](CH_3OH)(ClO_4)_2$ (**2**). Displacement ellipsoids are drawn at the 50% probability level. Carbon-bound hydrogen atoms, counter ions and solvent molecules are omitted for clarity

sites with various close to degenerate minima, and subtle effects due to secondary interactions, enforced by the slightly different environment, caused by the different ligand configurations, lead to the stabilization of the observed minimum structures.

Also of interest is the observation that the structural parameters of both isomers are different from those observed in the crystals; this was expected since with distances of significantly larger than 10 Å, the two $S = 1/2$ centers are expected to behave as (nearly) independent centers. According to the spectra simulations, the copper–copper distances are shortened in both isomers by 1–2 Å (see Tables 1, 2). This indicates that there are some conformational changes for **1** and **2** when these complexes are dissolved, and this is also apparent from the angles used in the spectra simulations (see Table 2). Similar observations have been made in other systems before, and these suggest that intermolecular interactions in the crystal lattices as well as in solution are of importance [13].

Experimental

Materials and instrumentation

The tridentate ligand L^1 [2-(3-methyl-3-(pyridin-2-yl)az-etidin-1-yl)ethanamine] was prepared as described previously [1]. For ion exchange chromatography the Na$^+$ form of SP Sephadex C-25 cation exchange resin was used. Reagents were purchased from Aldrich and used as purchased.

Electronic absorption spectra were measured with a SCINCO S-2100 diode array spectrophotometer. *IR spectra* (KBr pellets) were obtained with a JASCO 715 spectrometer. ^1H *NMR spectra* (in CDCl$_3$) were recorded on a Bruker Advance Digital 400 instrument. *X-band EPR spectra* (approx. 9.4 GHz) were recorded on a Bruker ELEXSYS E500 EPR spectrometer, equipped with a Super High Q Cavity. The temperature was held at 120 K using a flow cryostat with liquid nitrogen and a Eurotherm
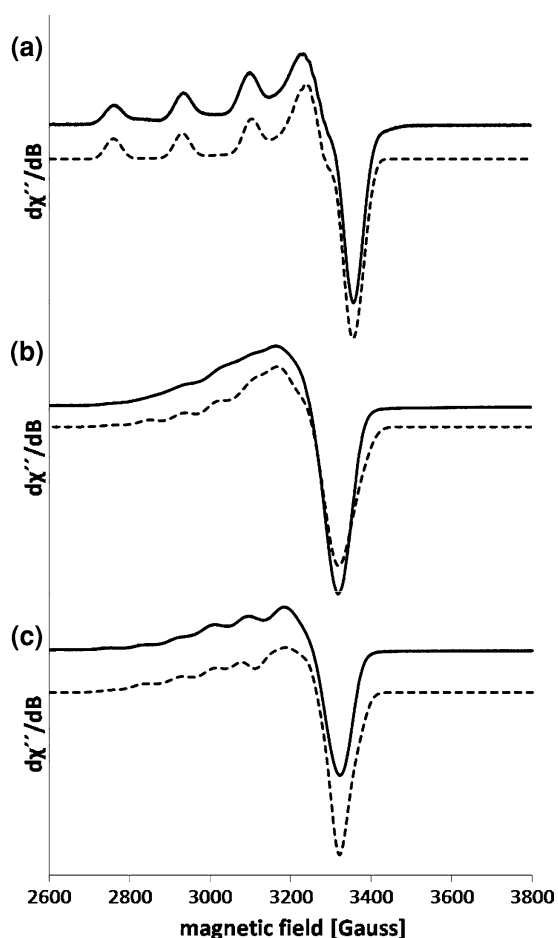
Fig. 3 Experimental (full line, ca. 0.5 mM in DMF/H_2O = 3:2, ca. 120 K) and simulated (dashed line) [14, 15] EPR spectra of **a** mononuclear $[(L^1)Cu(Cl)_2]$ (9.434575 GHz), **b** dinuclear $[(L^2)Cu_2(Cl)_3(OH)]$ (9.437620 GHz), and **c** dinuclear $[(L^3)Cu_2(Cl)_2(OH_2)_2]^{2+}$ (9.437052 GHz)

used [14, 15]. Elemental analyses, using a Vario EL elemental analysis apparatus (Elementar), were obtained from the microanalytical laboratories of the chemistry department of the University of Heidelberg.

Syntheses

$[(Cl)_2(Cu(L^2))Cu(Cl)(OH)]\cdot H_2O$ (**1**)

Isophthalaldehyde (0.18 g) was added to L^1 (0.53 g) in absolute ethanol (50 mL) and the mixture was stirred at room temperature for 1 h then heated under nitrogen at 70 °C for 24 h. It was cooled to room temperature, evaporated under reduced pressure, and dissolved in methanol (100 mL), before cooling to ~ 5 °C in an ice bath. $NaBH_4$ (1.0 g) was gradually added with stirring. Stirring was continued overnight at room temperature, then 2 mol L^{-1} HCl (10 mL) was added and stirring continued for a further 2 h. The solution was evaporated to dryness and 1 mol L^{-1} NaOH (100 mL) was added. This mixture was extracted with chloroform (30 mL × 3), and the chloroform extracts were washed with water (50 mL × 3), dried with anhydrous Na_2SO_4, then evaporated under reduced pressure to give a light brown oil (0.60 g), L^2. The crude ligand (0.60 g) in methanol (50 mL) was mixed with $CuCl_2\cdot 2H_2O$ (0.42 g) in methanol (30 mL), and the resulting homogeneous blue solution was evaporated to dryness. The residue was dissolved in water (200 mL), adsorbed onto SP Sephadex C-25 and eluted with 0.3 mol L^{-1} NaCl. The major blue band eluate (followed by a minor green band) was evaporated to dryness. The complex was extracted into ethanol, leaving a residue of NaCl. Evaporation of the ethanol extract gave 0.60 g of a blue powder. Crystals suitable for a structure determination were obtained by slow recrystallization of an ethanolic solution of this product. Anal. Calcd. for $C_{30}H_{52}Cl_4Cu_2N_6O_{10}$: C, 38.93; H, 5.66; N, 9.08. Found: C, 38.68; H, 5.55; N, 9.09%. IR spectrum (KBr pellet/cm^{-1}): 3430 (OH), 3175 (NH) cm^{-1}. Electronic spectrum (in water): $\lambda_{max} = 649.5$ nm, log $\varepsilon_{max} = 2.44$.

(B-VT-2000) temperature controller. A 3:2 mixture of DMF and water was used as solvent in all cases. Visualization of the spectra was done with the programme package Xepr-XeprView (version 2.4b.12), and for simulation of the spectra the software package XSophe-Sophe-XEprView (version 1.1.4) and MoSophe (version 2.0.91) were

Table 2 Spin Hamiltonian and structural parameters used for the simulation of the EPR spectra

	$[(L^1)Cu(Cl)_2]$	$[(L^2)Cu_2(Cl)_3(OH)]$ (**1**)	$[(L^3)Cu_2(Cl)_2(OH_2)_2]^{2+}$ (**2**)
g (x, y, z)	2.070, 2.038, 2.233	2.080, 2.041, 2.231	2.120, 2.052 (2.042), 2.231
A (x, y, z) [G]	17, 16, 179	22, 25, 175	12, 17, 181
Angle (α, β) [°]^a	–	10, 30	0, 20
Cu–Cu [Å]	–	8.8	9.2
J [cm^{-1}]	–	−0.50	−0.37

^{a} α and β are defined as in Table 1 except that here, these are the angles related to the g-tensors of Cu_1 and Cu_2; it appears that the g-tensor axes generally are approximately parallel to the structural Cartesian coordinate systems and the small deviations are generally neglected when simulated spectra are used to determine solution structures [8–12]

Table 3 Crystal data and structure refinement details

Compound	$[(Cl_2)Cu(L^2)Cu(Cl)(OH)]\cdot H_2O$ (**1**)	$[(Cl)(OH_2)Cu_2(L^3)(OH_2)(Cl)](CH_3OH)(ClO_4)_2$ (**2**)
Chemical formula	$C_{30}H_{43}Cl_3Cu_2N_6O_2$	$C_{31}H_{48}Cl_4Cu_2N_6O_{11}$
M/g mol^{-1}	753.13	949.63
Crystal system	Triclinic	Triclinic
Space group	$P\bar{1}$	$P\bar{1}$
a/Å	7.9713(4)	8.3331(5)
b/Å	12.4675(10)	10.4008(8)
c/Å	21.3127(18)	12.6238(11)
α/°	74.410(4)	69.250(4)
β/°	82.101(5)	77.667(5)
γ/°	74.395(4)	85.337(5)
V/Å^3	1,960.1(3)	999.52(13)
D_c/g cm^{-3}	1.276	1.578
Z	2	1
F(000)	780	490
$\mu(MoK_\alpha)$/mm^{-1}	1.321	1.394
$T_{min,max}$	0.734, 0.936	0.755, 0.894
hkl range	$-9 \leq h \leq 9$, $-15 \leq k \leq 15$, $-25 \leq l \leq 25$	$-10 \leq h \leq 10$, $-12 \leq k \leq 12$, $-15 \leq l \leq 15$
N	66,392	28,892
N_{ind} (R_{merge})	7,412 (0.047)	3,755 (0.028)
N_{obs} ($I > 2\sigma(I)$)	5,795	3,257
N_{par}	390	254
$R_1(F)$	0.085	0.070
$wR_2(F^2)$	0.258	0.176
GoF(all)	1.064	1.091
$\Delta\rho_{min}/e$Å^3	-0.62	-2.09
$\Delta\rho_{max}/e$Å^3	1.81	1.92

$[(Cl)(OH_2)Cu_2(L^3)(OH_2)(Cl)](CH_3OH)(ClO_4)_2$ (2)

Ligand L^3 (yield, 0.62 g) and its Cu(II) complex were prepared similar to that described above for L^2 but using terephthalaldehyde. A fast-eluting major blue band (followed by a weak green band) was again separated by chromatography on SP Sephadex and treated as described above. Yield, 0.60 g. Crystals suitable for a structure determination were obtained by slow evaporation of a methanolic solution of the complex in presence of an excess of LiClO$_4$. Anal. Calcd. for $C_{32}H_{49}Cl_3Cu_2N_6O_{14}$: C, 39.41; H, 5.06; N, 8.62. Found: C, 39.58; H, 5.17; N, 8.77%. IR (KBr pellet/cm^{-1}): 3442 (br) (OH), 3176 (NH), ClO$_4$ 1094 (br). Visible spectrum (in water): $\lambda_{max} = 653.5$ nm, log $\varepsilon_{max} = 2.47$.

Crystallography

The data were collected at 100(2) K on a Nonius Kappa-CCD area detector diffractometer [16] using graphite-monochromated Mo-K_α radiation (λ 0.71073 Å). The crystals were introduced in glass capillaries with a protecting "Paratone-N" oil (Hampton Research) coating. The unit cell parameters were determined from 10 frames, then refined on all data. The data (combinations of φ- and ω-scans giving complete data sets up to $\theta = 25.7°$ and a minimum redundancy of 4 for 90% of the reflections) were processed with HKL2000 [17]. The structures were solved by direct methods (1) or Patterson map interpretation (2) with SHELXS-97 and subsequent Fourier-difference synthesis, and refined by full-matrix least-squares on F^2 with SHELXL-97 [18]. Absorption effects were corrected empirically with the program SCALEPACK [17]. All non-hydrogen atoms were refined with anisotropic displacement parameters. The carbon-bound hydrogen atoms were introduced at calculated positions and were treated (as well as the oxygen- and nitrogen-bound hydrogen atoms when found) as riding atoms with an isotropic displacement parameter equal to 1.2 (OH, NH, CH, CH$_2$) or 1.5 (CH$_3$) times that of the parent atom. Specific details are as follows:

Complex **1**. The oxygen-bound hydrogen atoms were neither found, nor introduced, and the nitrogen-bound ones were introduced at calculated positions. Very large voids in

the lattice indicate the presence of unresolved solvent (probably water) molecules. The corresponding density has been taken into account with the program SQUEEZE in PLATON [19].

Complex **2**. The solvent methanol molecule, being too close to its image by symmetry, has been given an occupancy parameter of 0.5. The oxygen- and nitrogen-bound hydrogen atoms were found on a Fourier-difference map, except for that of the solvent methanol molecule.

Crystal data and structure refinement details are given in Table 3, and selected bond lengths and angles are presented in Table 2. The molecular plots were drawn with SHELXTL [18]. CCDC-735333 (**1**) and 735334 (**2**) contain the supplementary crystallographic data for this paper. These data can be obtained free of charge via www.ccdc.cam.ac.uk.

References

1. Lee, Y.H., Harrowfield, J., Kim, Y., Lim, W.T., Park, Y.C., Thuéry, P.: Functionalised azetidines as ligands: species derived by selective alkylation at substituent-nitrogen. Dalton Trans. **3**, 443–454 (2009)

2. Bernhardt, P.V., Cho, J.H., Harrowfield, J.M., Kim, J.Y., Kim, Y., Thuéry, S.P., Yoon, D.C.: Polyamines from polyols–pathways to azamacrocycles with hydroxymethyl pendent groups. Polyhedron **25**, 1811–1822 (2006)

3. Meyerstein, D.: Are M–N bonds indeed inherently weaker when N is a tertiary rather than a primary or secondary nitrogen atom? Coord. Chem. Rev. **185–186**, 141–147 (1999)

4. Harrowfield, J.M., Jang, G.H., Kim, Y., Thuéry, P., Vicens, J.: Azetidines as intermediates in polyamine synthesis - structure and reactions of a quadridentate ligand incorporating an azetidine ring. J. Chem. Soc., Dalton Trans. **7**, 1241–1243 (2002)

5. Keller, L., Sanchez, M.V., Prim, D., Couty, F., Evano, G., Marrot, J.J.: Azetidines as ligands in the Pd(II) complexes series. Organomet. Chem. **690**, 2306–2311 (2005)

6. Addison, A.W., Rao, T.N., Reedijk, J., van Rijn, J., Verschoor, G.: Synthesis, structure, and spectroscopic properties of copper(II) compounds containing nitrogen-sulfur donor ligands: the crystal and molecular structure of aqua[1,7-bis(N-methyl-benzimidazol-2'-yl)-2,6-dithiaheptane]copper(II) perchlorate. J. Chem. Soc. Dalton Trans. 1349–1356 (1984)

7. Smith, T.D., Pilbrow, J.R.: The determination of structural properties of dimeric transition metal ion complexes from EPR. Coord. Chem. Rev. **13**, 173 (1974)

8. Bernhardt, P.V., Comba, P., Hambley, T.W., Massoud, S.S., Stebler, S.: Molecular mechanics calculations of transition metal complexes. Inorg. Chem. **31**, 2644–2651 (1992)

9. Comba, P., Hilfenhaus, P.: One-step template synthesis and solution structures of bis(macrocyclic) octaamine dicopper(II) complexes. J. Chem. Soc., Dalton Trans. **20**, 3269–3274 (1995)

10. Comba, P., Hambley, T.W., Hilfenhaus, P., Richens, D.T.: Solid state and solution structures of two structurally related dicopper complexes with markedly different redox properties. J. Chem. Soc., Dalton Trans. 533–539 (1996)

11. Comba, P., Cusack, R., Fairlie, D.P., Gahan, L.R., Hanson, G.R., Kazmaier, U., Ramlow, A.: The solution structure of a copper(II) compound of a new cyclic octapeptide by EPR spectroscopy and force field calculations. Inorg. Chem. **37**, 6721–6727 (1998)

12. Comba, P., Lampeka, Y.D., Prikhod'ko, A., Rajaraman, G.: Determination of the solution structures of melamine-based bis- and tris-macrocyclic ligand copper(II) complexes. Inorg. Chem. **45**, 3632–3638 (2006)

13. Comba, P., Kerscher, M., Lampeka, Y.D., Lötzbeyer, L., Pritzkow, H., Tsymbal, L.V.: Structural properties of cyclopentanone-bridged bis-macrocyclic ligand dicopper (II) complexes in the solid and in solution: a successful test of the MM-EPR method. Inorg. Chem. **42**, 3387–3389 (2003)

14. Wang, D., Hanson, G.R.: A new method for simulating randomly oriented powder spectra in magnetic resonance: the Sydney Opera House (SOPHE) method. J. Magn. Reson. A **117**, 1–8 (1995)

15. Hanson, G.R., Gates, K.E., Noble, C.J., Griffin, M., Mitchell, A., Benson, S.J.: XSophe-Sophe-XeprView. A computer simulation software suite (v. 1.1.3) for the analysis of continuous wave EPR spectra. Inorg. Biochem. **98**, 316–903 (2004)

16. Hooft, R.W.W.: COLLECT, Nonius BV. Delft, The Netherlands (1998)

17. Otwinowski, Z., Minor, W.: Processing of x-ray diffraction data collected in oscillation mode. Methods Enzymol. **276**, 307–326 (1997)

18. Sheldrick, G.M.: A short history of SHELX. Acta Crystallogr. **A64**, 112 (2008)

19. Spek, A.L.: Single-crystal structure validation with the program PLATON. J. Appl. Crystallogr. **36**, 7 (2003)